


Performance optimization of continuous-variable quantum teleportation with generalized photon-varying non-Gaussian operations

Mingjian He^{✉*} and Shouyin Liu[†]*College of Physical Science and Technology, Central China Normal University, Wuhan, Hubei 430079, China* (Received 7 February 2024; revised 19 May 2024; accepted 14 June 2024; published 9 July 2024)

Continuous variable quantum teleportation provides a path to the long-distance transmission of quantum states. Photon-varying non-Gaussian operations have been shown to improve the fidelity of quantum teleportation when integrated into the protocol. However, for a given type of non-Gaussian operation, the achievable fidelity varies with the parameters associated with the operation. Previous work only focused on particular settings of the parameters, over which an optimization was missing. The potential of such operations is not fully uncovered. Given a fixed non-Gaussian operation, the achievable fidelity also varies with input states. An operation that increases the fidelity for teleporting one class of states might do the contrary for other classes of states. A performance metric, upon which an operation is optimized, suitable for different input states, is also missing. In this work, we build a framework for photon-varying non-Gaussian operations for multimode states, upon which we propose a performance metric suitable for arbitrary teleportation input states. We then apply the new metric to evaluate different types of non-Gaussian operations. Starting from simple multiphoton photon subtraction and photon addition, we find that increasing the number of ancillary photons involved in the operation does not guarantee performance improvement. We then investigate a generalization of the operations mentioned above, finding that operations that approximate a particular form provide the best improvement. The results provided here will be valuable for real-world implementations of quantum teleportation networks and applications that harness the non-Gaussianity of quantum states.

DOI: [10.1103/PhysRevA.110.012425](https://doi.org/10.1103/PhysRevA.110.012425)

I. INTRODUCTION

Continuous variable (CV) quantum teleportation protocols, adaptable with off-the-shelf optical technologies, provide a path to the long-distance transmission of quantum information encoded in quantum states. Many breakthroughs have been made in the deployment of large-scale quantum teleportation systems over the past decades, e.g., [1–6].

The core of teleportation is the consumption of entangled *resource states* distributed before the protocol begins. However, imperfect resource states caused by finite power during state production and channel loss during state distribution limit the achievable fidelity of the *input state* (the state to be teleported). One class of resource states is the two-mode squeezed vacuum (TMSV) state, which can be produced by combining two single-mode squeezed vacuum states at a balanced beam splitter. Perfect teleportation requires TMSV states with infinite squeezing, which is unachievable in theory and experiment (e.g., only 15-dB squeezing is achievable with state-of-the-art technologies [7]). TMSV states with

higher squeezing are also more sensitive to decoherence during distribution over lossy channels [8], making the long-distance distribution of TMSV states another outstanding challenge.

Non-Gaussian operations have been shown to enhance entanglement and other desirable properties when applied to Gaussian states. Much attention has been drawn to the studies of such operations in various quantum information applications, such as quantum key distribution [9–20], noiseless linear amplification [21–27], entanglement distillation [28–35], and quantum computing [36–39]. In teleportation, non-Gaussian operations can improve fidelity at the cost of reduced overall efficiency, e.g., [40–56]. However, for a given type of non-Gaussian operation, the achievable fidelity varies with the parameters associated with the operation. For example, varying the number of photons being subtracted (or added) in photon subtraction (or addition) provides different fidelity [44–47]. The fidelity offered by a cascaded application of the same operation also varies with the number of operations [55]. Previous work focused on particular parameter settings, e.g., restricting the number of ancillary photons in the operation or the number of cascaded operations to a few (mostly ≤ 3 for [40–56]). It remains unclear whether increasing the complexity of non-Gaussian operations always improves fidelity. To fully reveal the potential of non-Gaussian operations, an optimization over the parameters of the operations is needed.

To carry out the optimization a proper performance metric is also needed. Previous work focused on the fidelity of

*Contact author: mingjian.he@ccnu.edu.cn†Contact author: syliu@ccnu.edu.cn

Published by the American Physical Society under the terms of the Creative Commons Attribution 4.0 International license. Further distribution of this work must maintain attribution to the author(s) and the published article's title, journal citation, and DOI.

particular classes of input states, e.g., coherent states, squeezed states, and CV qubit states. However, for a given resource state, the achievable fidelity also varied with different input states. The fidelity for teleporting one input state cannot properly gauge the performance of teleporting other input states. For example, for coherent states input, applying photon subtraction to the resource states increases fidelity [40] while using photon addition decreases the fidelity [41]. On the contrary, for squeezed states input, applying photon subtraction and photon addition both increase the fidelity [42]. The energy-constrained channel fidelity was proposed in [57] and developed in [58] as a performance metric for teleportation. However, the metric is independent of the input states and does not indicate the achievable fidelity for any input states. A performance metric suitable for different input states is still missing.

This paper aims to fully uncover the potential of the photon-varying (PV) operations (i.e., operations that include both photon subtraction and photon addition) in CV teleportation. To this end, we first build a framework for PV operations in the multimode setting, expressing the characteristic function of the photon-varied state as a multivariable multi-index Hermite-Gaussian function. Based on the framework built, we introduce a performance metric suitable for arbitrary input states. We then propose generalized PV operations with parameters optimized using the new metric as the cost function. Using practical photon catalysis as an example, we also demonstrate possible methods to implementing the generalized operations. Our results show that the optimal generalized PV operations approach a specific Gaussian operation, the noiseless linear amplification. The key contributions of this paper are summarized as follows.

(i) We derive an analytical solution to the characteristic functions of multimode Gaussian state modified by PV operations.

(ii) Using the new solution, we propose a new performance metric for PV operations in CV teleportation. With the metric, we explain why PV operations provide different fidelity improvements for different input states. We also show that PV operations do not always provide increasing fidelity as the complexity of the operations grows.

(iii) We propose a generalized PV operation. Optimizing the operation against the metric we show that such an operation always provides increasing fidelity as the complexity of the operation grows.

The analytical solution we derived is of independent interest in its own right. Compared with a similar solution in [53], our solution does not contain any differential operators and is compatible with multimode Gaussian states. We expect the solution to be useful also for other quantum information applications that benefit from multimode non-Gaussian operations, e.g., measurement-based quantum computation [59] and cluster states teleportation [60].

The remaining sections are organized as follows. Section II establishes a framework for CV teleportation with TMSV resource states and photon-varying operations, upon which the generalized photon-varying operations are introduced and investigated in Sec. III. Section IV extends the studies of the above operations in teleportation with generalized TMSV states. Conclusions of the paper are given in Sec. V.

II. CV TELEPORTATION WITH PHOTON-VARYING OPERATIONS

We consider the Vaidman-Braunstein-Kimble (VBK) protocol, which is the first CV teleportation protocol proposed in [61] and developed in [62]. In the VBK protocol, Alice first prepares a TMSV state with modes 1 and 2 and sends mode 2 to Bob. The distributed state is then used as the resource state for teleportation. Alice couples the input mode (to which the input state is encoded) with mode 1 at a balanced beam splitter. The p quadrature of one output of the beam splitter and the q quadrature of the other output are measured by two homodyne detectors. The measurement outcome is sent to Bob through a lossless classical channel. Based on the outcome received, Bob applies a displacement operation to mode 2. In the limit of infinite squeezing of the resource state, mode 2 approaches the input mode.

We define the Wigner characteristic function (CF) of a single-mode state with density operator $\hat{\rho}$ as

$$\chi(\xi) = \text{tr}\{\hat{\rho}\hat{D}(\xi)\}, \quad (1)$$

where $\xi \in \mathbb{C}$, $\text{tr}\{\cdot\}$ represents the trace operation, $\hat{D}(\xi) = e^{\xi\hat{a}^\dagger - \xi^*\hat{a}}$ is the displacement operator, \hat{a} and \hat{a}^\dagger are the ladder operators of $\hat{\rho}$, and $(\cdot)^*$ represents the complex conjugate. The relation between the input and output modes of the VBK protocol can be described using the CF formalism [63]

$$\chi_{\text{out}}(\xi) = \chi(\xi, \xi^*)\chi_{\text{in}}(\xi), \quad (2)$$

where $\chi_{\text{in}}(\xi)$ is the CF of the input mode, $\chi_{\text{out}}(\xi)$ is the CF of the output mode (averaged over Alice's measurement outcomes), and $\chi(\xi_1, \xi_2)$ is the CF of the resource state. The above equation indicates that the protocol can be viewed as a quantum channel with a ξ -dependent *response function* $\chi(\xi, \xi^*)$. The output mode after passing the quantum channel approaches the input mode when the response function is flat, i.e., $\chi(\xi, \xi^*) \rightarrow 1$ for all ξ . The performance of teleportation can be measured by the fidelity between the input mode and the output mode, which quantifies the closeness of the CFs of the two modes [64]

$$\mathcal{F} = \frac{1}{\pi} \int d^2\xi \chi_{\text{in}}(-\xi)\chi_{\text{out}}(\xi), \quad (3)$$

where $d^2\xi := d\xi \wedge d\xi^*$ with \wedge the exterior product. The fidelity approaches unit for any input states when the response function $\chi(\xi, \xi^*) \rightarrow 1$.

Photon subtraction (\hat{a}^n , $n \in \mathbb{N}$) and photon addition ($\hat{a}^{\dagger n}$, $n \in \mathbb{N}$) are two types of non-Gaussian operations, both shown to improve the teleportation fidelity for certain input states. In [65] the states applied by the two operations mentioned above are named as photon-varied quantum states. In this paper, we will use photon-varying (PV) operations to refer to the two operations. A physical implementation to the PV operations is shown in Fig. 1(a), which consists of an ancillary Fock state $|l\rangle$, a photon number resolving detector, and a beam splitter with transmissivity $T < 1$. In the operation, the initial mode is coupled with the ancillary state at the beam splitter. A photon number-resolving detection is performed on one output of the beam splitter. The operation has been successful if m photons are detected. Photon subtraction \hat{a}^n can be approximated by setting $l = 0$, $m = n$, and $T \rightarrow 1$ while photon

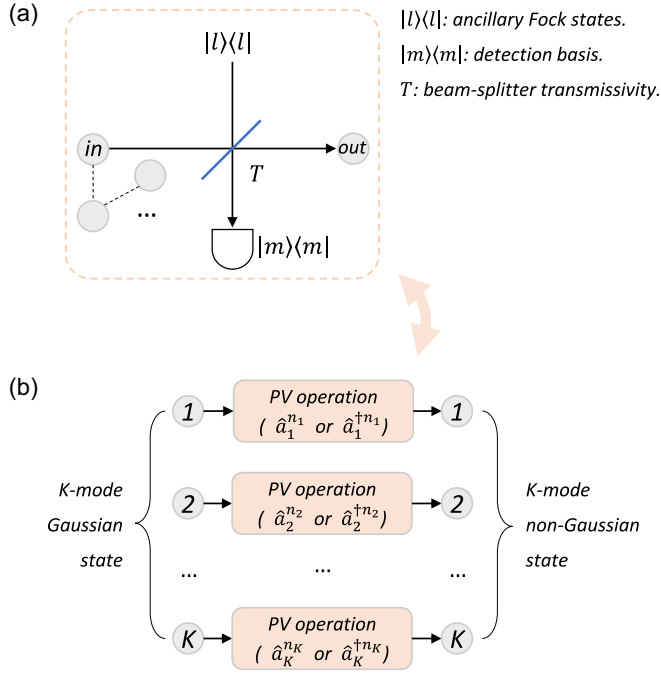


FIG. 1. (a) A physical implementation to the PV operations. (b) The application of K PV operations to a K -mode Gaussian state.

addition $\hat{a}^{\dagger n}$ can be approximated by setting $l = n$, $m = 0$, and $T \rightarrow 1$. Both operations can also be implemented by a cascaded applications of the same single-photon operations.

The transformation for performing a PV operation on the single-mode state $\hat{\rho}$ can be written as

$$\hat{\rho} \rightarrow \hat{\rho}_{\text{PV}} = \frac{1}{\text{tr}\{\hat{a}^n \hat{\rho} \hat{a}^{\dagger n}\}} \hat{a}^n \hat{\rho} \hat{a}^{\dagger n}, \quad (4)$$

where \hat{a} is replaced with \hat{a}^{\dagger} for photon addition. Using the identities

$$\begin{aligned} \text{tr}\{\hat{a} \hat{\rho} \hat{D}(\xi)\} &= -e^{-\frac{|\xi|^2}{2}} \frac{\partial}{\partial \xi^*} \left[e^{\frac{|\xi|^2}{2}} \chi(\xi) \right], \\ \text{tr}\{\hat{\rho} \hat{a}^{\dagger} \hat{D}(\xi)\} &= e^{-\frac{|\xi|^2}{2}} \frac{\partial}{\partial \xi} \left[e^{\frac{|\xi|^2}{2}} \chi(\xi) \right], \\ \text{tr}\{\hat{a}^{\dagger} \hat{\rho} \hat{D}(\xi)\} &= e^{\frac{|\xi|^2}{2}} \frac{\partial}{\partial \xi} \left[e^{-\frac{|\xi|^2}{2}} \chi(\xi) \right], \\ \text{tr}\{\hat{\rho} \hat{a} \hat{D}(\xi)\} &= -e^{\frac{|\xi|^2}{2}} \frac{\partial}{\partial \xi^*} \left[e^{-\frac{|\xi|^2}{2}} \chi(\xi) \right], \end{aligned} \quad (5)$$

the transformation in Eq. (4) can be rewritten in an equivalent CF form as

$$\chi(\xi) \rightarrow \chi_{\text{PV}}(\xi) = \frac{1}{\mathcal{N}} O_{t,n}(\xi) \chi(\xi), \quad (6)$$

where

$$O_{t,n}(\xi) = (-1)^n e^{t \frac{|\xi|^2}{2}} \frac{\partial^{2n}}{\partial \xi^n \partial \xi^{*n}} e^{-t \frac{|\xi|^2}{2}}, \quad (7)$$

$\mathcal{N} = O_{t,n}(\xi) \chi(\xi)|_{\xi=0}$ is the normalization constant, $t = -1$ for photon subtraction, and $t = 1$ for photon addition. In [65] it was shown that the operator $O_{t,n}(\xi)$ can be simplified to a generalized two-variable Hermite polynomial function when

the initial state is a *single-mode* Gaussian state. To find the simplified form of the CF of the TMSV state after the PV operation, we first extend the result in [65] to the general multimode case.

For a symmetric $2K$ -by- $2K$ matrix \mathbf{M} , we define the generalized multi-index multivariable Hermite function by the generating function

$$\sum_{n_1, \dots, n_{2K}=0}^{\infty} \left(\prod_{i=1}^{2K} \frac{u_i^{n_i}}{n_i!} \right) H_{n_1, \dots, n_{2K}}(\mathbf{x}; \mathbf{M}) = e^{\mathbf{u}^T \mathbf{M} \mathbf{u} + \mathbf{x}^T \mathbf{u}}, \quad (8)$$

where $\mathbf{x}, \mathbf{u} \in \mathbb{C}^{2K}$ are column vectors, the u_i 's are elements of \mathbf{u} , and $(\cdot)^T$ represents matrix transpose (not conjugate transpose). Performing some algebraic manipulation on Eq. (8) leads to the analytical solution to $H_{n_1, \dots, n_{2K}}(\mathbf{x}; \mathbf{M})$,

$$\begin{aligned} H_{n_1, \dots, n_{2K}}(\mathbf{x}; \mathbf{M}) &= \sum_{\{n_{i,j}\}} \left[\prod_{i=1}^{2K} \frac{n_i! x_i^{q_i}}{q_i!} \frac{M_{i,i}^{n_{i,i}}}{n_{i,i}!} \prod_{j=i+1}^{2K} \frac{(2M_{i,j})^{n_{i,j}}}{n_{i,j}!} \right], \end{aligned} \quad (9)$$

where the $M_{i,j}$'s are elements of the matrix \mathbf{M} , the x_i 's are elements of the vector \mathbf{x} , the summation is taken over all possible combinations of the $n_{i,j}$'s ($1 \leq i \leq 2K$, $i \leq j \leq 2K$) such that $q_i \geq 0$ for all i , where

$$q_i = n_i - n_{i,i} - \sum_{i'=1}^{2K} n_{\min(i,i'), \max(i,i')}. \quad (10)$$

The details of the derivation of Eq. (9) can be found in Appendix A.

From Eq. (8) it follows that for a column vector $\mathbf{d} \in \mathbb{C}^{2K}$,

$$\begin{aligned} \sum_{n_1, \dots, n_{2K}=0}^{\infty} \left(\prod_{i=1}^{2K} \frac{u_i^{n_i}}{n_i!} \right) H_{n_1, \dots, n_{2K}}(\mathbf{M} \mathbf{x} - \mathbf{d}; -\frac{1}{2} \mathbf{M}) & \times e^{-\frac{1}{2} \mathbf{x}^T \mathbf{M} \mathbf{x} + \mathbf{d}^T \mathbf{x}} \\ &= e^{-\frac{1}{2} (\mathbf{x} - \mathbf{u})^T \mathbf{M} (\mathbf{x} - \mathbf{u}) + \mathbf{d}^T (\mathbf{x} - \mathbf{u})}. \end{aligned} \quad (11)$$

Comparing the terms in the Taylor expansion for the right side of the above equation it follows that

$$\begin{aligned} \frac{\partial^{\sum_{i=1}^{2K} n_i}}{\prod_{i=1}^{2K} (\partial x_i)^{n_i}} e^{-\frac{1}{2} \mathbf{x}^T \mathbf{M} \mathbf{x} + \mathbf{d}^T \mathbf{x}} &= (-1)^{\sum_{i=1}^{2K} n_i} H_{n_1, \dots, n_{2K}}(\mathbf{M} \mathbf{x} - \mathbf{d}; -\frac{1}{2} \mathbf{M}) e^{-\frac{1}{2} \mathbf{x}^T \mathbf{M} \mathbf{x} + \mathbf{d}^T \mathbf{x}}. \end{aligned} \quad (12)$$

The details of the derivation of Eq. (12) can also be found in Appendix A.

A K -mode Gaussian state with covariance matrix \mathbf{V} and vector of means $\boldsymbol{\mu}$ (\mathbf{V} and $\boldsymbol{\mu}$ are both for the quadratures) has the CF

$$\chi(\boldsymbol{\xi}) = e^{-\frac{1}{2} \tilde{\boldsymbol{\xi}}^{\dagger} \tilde{\mathbf{V}} \tilde{\boldsymbol{\xi}} + \tilde{\boldsymbol{\mu}}^{\dagger} \tilde{\boldsymbol{\xi}}}, \quad (13)$$

where $\boldsymbol{\xi} = [\xi_1, \dots, \xi_K] \in \mathbb{C}^K$, $\tilde{\boldsymbol{\xi}} = [\xi_1, \xi_1^*, \dots, \xi_K, \xi_K^*]^{\dagger}$ is the augmented vector of $\boldsymbol{\xi}$, $\tilde{\mathbf{V}} = \mathbf{Z} \mathbf{V} \mathbf{J} \mathbf{J}^{\dagger} \mathbf{Z}$, $\tilde{\boldsymbol{\mu}} = \mathbf{Z} \boldsymbol{\mu}$, $\mathbf{Z} = \mathbf{I}_K \otimes [1, 0; 0, -1]$, $\mathbf{J} = \mathbf{I}_K \otimes [1, i; 1, -i]/2$, \mathbf{I}_K is the K -by- K identity matrix, and we set the variance of the vacuum state to 1 shot noise unit (i.e., $\hbar = 2$) and will use this setting

throughout the paper. As shown in Fig. 1(b), suppose every mode of the K -mode state undergoes an independent PV operation with n_i ($1 \leq i \leq K$) photons varied. Combining Eqs. (6) and (12), the CF for the state after the operations can then be written as

$$\chi_{\text{PV}}(\xi) = \frac{(-1)^{\sum_{i=1}^K n_i}}{\mathcal{N}} H_{n_1, n_1, \dots, n_K, n_K} \left(\mathbf{X}(\tilde{\mathbf{V}}' \tilde{\xi} + \tilde{\mu}); -\frac{1}{2} \mathbf{X} \tilde{\mathbf{V}}' \right) \times \chi(\xi), \quad (14)$$

where $\tilde{\mathbf{V}}' = \tilde{\mathbf{V}} + \text{diag}[t_1, t_1, \dots, t_K, t_K]/2$, $t_i = -1$ (or 1) when photon subtraction (or photon addition) is applied to the i th mode, $\mathbf{X} = \mathbf{I}_K \otimes [0, 1; 1, 0]$, and

$$\mathcal{N} = (-1)^{\sum_{i=1}^K n_i} H_{n_1, n_1, \dots, n_K, n_K} \left(\mathbf{X} \tilde{\mu}; -\frac{1}{2} \mathbf{X} \tilde{\mathbf{V}}' \right). \quad (15)$$

For conciseness, we will use $H_{n_1, n_1, \dots, n_K, n_K}(\xi)$ to represent $H_{n_1, n_1, \dots, n_K, n_K}(\mathbf{X}(\tilde{\mathbf{V}}' \tilde{\xi} + \tilde{\mu}); -\frac{1}{2} \mathbf{X} \tilde{\mathbf{V}}')$ in the rest of the paper when the context is clear.

We can now proceed with the two-mode case. Applying PV operations (with parameters n_1 and n_2 for the two modes, respectively) to both modes of a two-mode Gaussian state produces a photon-varied state with CF of the form

$$\chi_{\text{PV}}(\xi_1, \xi_2) = \frac{(-1)^{n_1+n_2}}{\mathcal{N}} H_{n_1, n_1, n_2, n_2}(\xi_1, \xi_2) \chi(\xi_1, \xi_2). \quad (16)$$

For an arbitrary input state, teleportation using the above state as resource state or using a resource state without any operation are equivalent to quantum channels with different response functions. The ratio between the two response functions can be written as

$$\frac{\chi_{\text{PV}}(\xi, \xi^*)}{\chi(\xi, \xi^*)} = \frac{1}{H_{n_1, n_1, n_2, n_2}(0, 0)} H_{n_1, n_1, n_2, n_2}(\xi, \xi^*) := \mathcal{H}(\xi). \quad (17)$$

The function $\mathcal{H}(\xi)$, which we name as the *response ratio* function, can be used to indicate the impact of the PV operations. The benefits of using the response ratio function are twofold. First, the response ratio function characterizes the resource states modified by PV operations and is independent of the input states, yet can be used to calculate the fidelity for any input states. Second, for Gaussian resource states, the response ratio functions associated with the PV operations are (normalized) Hermite polynomial functions, which have many well-studied properties that will help analyze the PV operations.

The response ratio functions directly reveal the impact of PV operations on the resource states. Recall from Eq. (2) the output state of teleportation with resource state modified by the PV operation can be written as

$$\chi_{\text{out}}(\xi) = \mathcal{H}(\xi) \chi(\xi, \xi^*) \chi_{\text{in}}(\xi). \quad (18)$$

For Gaussian resource state with response function $\chi(\xi, \xi^*) \in (0, 1)$, at any point ξ_p , $\mathcal{H}(\xi_p) > 1$ indicates that the PV operations reduce distortion caused by the quantum teleportation channel to any input state at ξ_p . Applying PV operations with $\mathcal{H}(\xi) > 1$ for all ξ to the resource state improves the teleportation fidelity for any input state. For PV operations with $\mathcal{H}(\xi) > 1$ only for a certain area of ξ , the increase in fidelity depends on the input state.

We now consider the TMSV state with the form

$$|\text{TMSV}\rangle = \hat{S}(r) |0, 0\rangle_{1,2} = \sqrt{1 - \lambda^2} \sum_{n=0}^{\infty} \lambda^n |n, n\rangle_{1,2}, \quad (19)$$

where $\hat{S}(r) = e^{r(\hat{a}_1^\dagger \hat{a}_2^\dagger - \hat{a}_1 \hat{a}_2)}$ is the two-mode squeezing operator and $r = \text{atanh}(\lambda)$ is the squeezing parameter. The CF of the TMSV state is then given by

$$\chi_{\text{TMSV}}(\xi_1, \xi_2) = e^{-\frac{1}{2}[V(|\xi_1|^2 + |\xi_2|^2) - \sqrt{V^2 - 1}(\xi_1 \xi_2 + \xi_1^* \xi_2^*)]}, \quad (20)$$

where $V = \cosh(2r)$ is the variance of the distribution of the quadratures. The response ratio function for the TMSV state with PV operations can be written as

$$\mathcal{H}(\xi) = H_{n_1, n_1, n_2, n_2}(\xi, \xi^*) / H_{n_1, n_1, n_2, n_2}(0, 0), \quad (21)$$

where

$$\begin{aligned} & H_{n_1, n_2, n_3, n_4}(\xi, \xi^*) \\ &= \sum_{n_5, n_6, n_7, n_8} \xi^{(n_2+n_3)} \xi^{*(n_1+n_4)} |\xi|^{2(-n_5-n_6-n_7-n_8)} \\ & \times \frac{n_1! n_2! (A+C)^{n_1+n_2-2n_5-n_7-n_8} A^{n_5}}{n_5! (n_1-n_5-n_7)! (n_2-n_5-n_8)!} \\ & \times \frac{n_3! n_4! (B+C)^{n_3+n_4-2n_6-n_7-n_8} B^{n_6} C^{n_7+n_8}}{n_6! (n_3-n_6-n_7)! (n_4-n_6-n_8)! n_7! n_8!}, \end{aligned} \quad (22)$$

the summation is taken over all possible n_i 's ($i = 5, 6, 7, 8$) such that the variables in every factorial are nonnegative, $A, B = -(V-1)/2$ for photon subtraction, $A, B = -(V+1)/2$ for photon addition (A and B can take different values when different operations are applied to the two modes), and $C = \sqrt{V^2 - 1}/2$ for both operations.

Figure 2 shows the response ratio function $\mathcal{H}(\xi)$ for PV operations with different settings. In this paper, the squeezing of TMSV states in the dB unit is $r_{\text{dB}} = -10 \log_{10}[\exp(-2r)]$. In Figs. 2(a) and 2(b), we consider scenarios where both modes of a TMSV state are applied with the same operation (i.e., the symmetric scenarios with $n_1 = n_2 = n$). For both PV operations the response ratios are functions of $|\xi|^2$. For photon subtraction, we find $\mathcal{H}(\xi) > 1$ for any ξ , showing that symmetric photon subtraction can improve teleportation fidelity for any input states. For photon addition $\mathcal{H}(\xi) < 1$ is found when $|\xi|^2$ is less than a certain threshold, indicating that symmetric photon addition cannot improve fidelity for input states with CF centered around the origin, e.g., coherent states and Fock states. For input states with CF spread across the complex plain, e.g., squeezed states with high squeezing, it is possible for symmetric photon addition to improve fidelity. For both PV operations, increasing n does not always increase $\mathcal{H}(\xi)$ for every ξ . In Fig. 2(c), we consider scenarios where different operations are applied to the modes, finding none of the asymmetric scenarios provide $\mathcal{H}(\xi)$ larger than their symmetric counterpart for any ξ . Although not shown in Fig. 2(c), we also compare the response ratio function $\mathcal{H}(\xi)$ with the above PV operations for TMSV states with different squeezing, finding that the above conclusions still hold but the scales are different.

We use coherent states as the input state to exemplify how the response ratio function connects with the

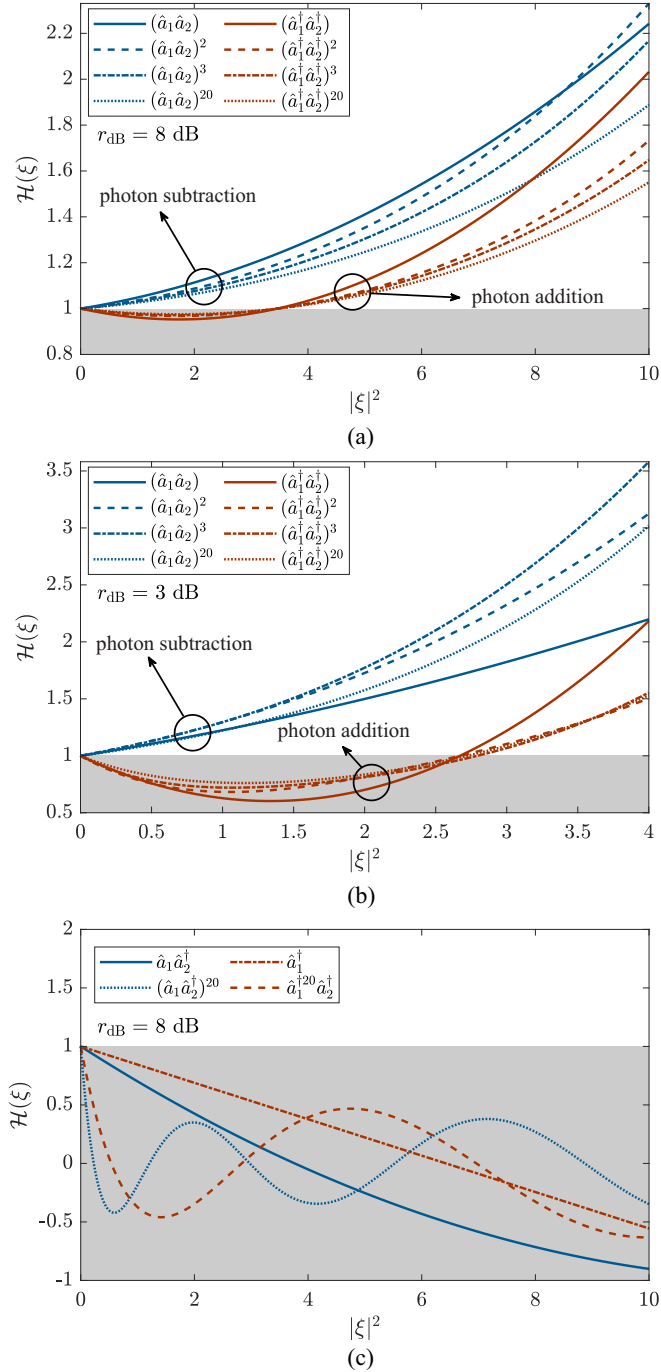


FIG. 2. The response ratio function $\mathcal{H}(\xi)$ for PV operations with different settings. The same operation is applied to both modes of a TMSV state with (a) 8-dB squeezing and (b) 3-dB squeezing. In (c), different PV operations are applied to the modes of the state. In this figure and the figures to follow, all axes are unitless.

teleportation fidelity. We note the transmission of coherent states is a critical step in various quantum information applications and methods to increase the transmission distance have been proposed over the past decade, e.g., using an ancillary TMSV state in an erasure-correcting code [66,67], measuring the environmental mode and performing local operations on the transmitted mode [68], and using teleportation enhanced

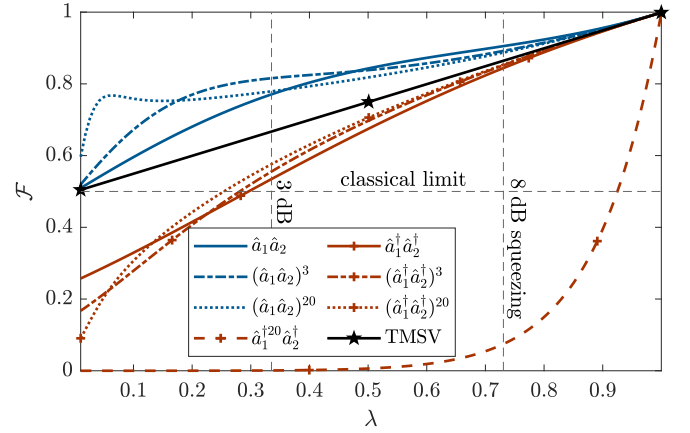


FIG. 3. The fidelity for teleportation of coherent states using TMSV states modified by PV operations. The horizontal line represents the $1/2$ classical limit for teleportation of coherent states. The vertical lines represent the squeezing of 3 dB and 8 dB (as indicated by the texts).

with the non-Gaussian operations discussed in this work. The CF for a coherent state $|\alpha\rangle$ is

$$\chi_{\text{coh}}(\xi) = e^{-\frac{1}{2}|\xi|^2 + \xi\alpha^* - \xi^*\alpha}. \quad (23)$$

The fidelity for teleportation using TMSV states modified by PV operation can then be written as

$$\mathcal{F} = \frac{1}{\pi} \int d^2\xi e^{-|\xi|^2} e^{-(V - \sqrt{V^2 - 1})|\xi|^2} \mathcal{H}(\xi). \quad (24)$$

Figure 3 compares the fidelity for teleportation of coherent states using TMSV states modified by different PV operations. When photon addition is applied to any mode of the TMSV state, the fidelity cannot be improved and even drops below the $1/2$ classical limit for certain λ . For photon subtraction, subtracting more photons is only effective when the initial squeezing is small.

III. CV TELEPORTATION WITH GENERALIZED PHOTON-VARYING OPERATIONS

For TMSV resource states, an upper bound to any $\mathcal{H}(\xi)$ can be written as

$$\mathcal{H}_{\text{max}}(\xi) = \frac{1}{\chi_{\text{TMSV}}(\xi, \xi^*)} = e^{(V - \sqrt{V^2 - 1})|\xi|^2}. \quad (25)$$

The response ratio functions $\mathcal{H}(\xi)$ associated with PV operations $\hat{a}_i^{n_i}$ and $\hat{a}_i^{\dagger n_i}$ ($i = 1, 2$) are both polynomial functions of $|\xi|^2$, of which the degree equals $n_1 + n_2$. We showed in the previous section that these functions did not approach $\mathcal{H}_{\text{max}}(\xi)$ with increasing degree. It remains unclear whether $\mathcal{H}(\xi)$ associated with combinations of the PV operations that approaches $\mathcal{H}_{\text{max}}(\xi)$ exists.

Consider one generalized PV operation \hat{A}_N^\dagger (with a conjugate transpose \hat{A}_N) of the form

$$\hat{A}_N^\dagger = \sum_{n=0}^N e_n \hat{a}_1^{\dagger n} \hat{a}_2^{\dagger n}, \quad (26)$$

where the e_n 's are normalized real-value coefficients. We note that the generalized PV operation defined above does not contain any asymmetric term as we showed in the previous section that asymmetric PV operations are inferior to their symmetric counterparts. The response ratio function for a TMSV state with the generalized PV operation given by Eq. (26) can be written as

$$\mathcal{H}(\xi) = \frac{1}{\mathbf{e}^T \mathbf{H}(0, 0) \mathbf{e}} \mathbf{e}^T \mathbf{H}(\xi, \xi^*) \mathbf{e}, \quad (27)$$

where $\mathbf{e} = [e_0, \dots, e_N]^T$,

$$\mathbf{H}(\xi, \xi^*) = \begin{bmatrix} H_{0,0,0,0}(\xi, \xi^*) & \dots & H_{N,0,N,0}(\xi, \xi^*) \\ \vdots & \ddots & \vdots \\ H_{0,N,0,N}(\xi, \xi^*) & \dots & H_{N,N,N,N}(\xi, \xi^*) \end{bmatrix}, \quad (28)$$

and the elements $H_{n_1, n_2, n_3, n_4}(\xi, \xi^*)$ are given by Eq. (22) [with $A = B = -(V + 1)/2$].

For given TMSV states, we use the integrated response ratio function as the target function to be maximized. For a fixed N , the optimization is taken over the vector \mathbf{e} . The optimal \mathbf{e} can then be written as

$$\mathbf{e}_{\text{opt}} = \underset{\mathbf{e} \in \mathbb{R}^{N+1}}{\text{argmax}} \int_0^{\xi_{\text{lim}}} \mathcal{H}(\xi) d|\xi|, \quad (29)$$

where we set an upper limit ξ_{lim} for the integration with respect to $|\xi|$. Figures 4(a) and 4(b) show the response ratio function $\mathcal{H}(\xi)$ for the generalized PV operations \hat{A}_N^\dagger with optimized parameters. In this paper, we adopt a particle swarm algorithm for all optimization problems. In Figs. 4(a) and 4(b) the parameter vector \mathbf{e} is set to maximize the integrated response ratio function (with $\xi_{\text{lim}} = 2$). Distinct from the PV operations discussed in the previous section, the generalized PV operations here always provide increasing $\mathcal{H}(\xi)$ with increasing N . The response ratio function also approaches the upper bound $\mathcal{H}_{\text{max}}(\xi)$ as N grows. However, we are unable to show that $\mathcal{H}_{\text{max}}(\xi)$ is saturated when N approaches infinite because we cannot optimize $\mathcal{H}(\xi)$ accurately with $N > 20$.

We attempt to better explain why the generalized PV operations provide increasing $\mathcal{H}(\xi)$ as the degree of the operations grows. The upper bound in Eq. (25) can be saturated by the noiseless linear amplifier (NLA), which is given by

$$g^{\hat{a}_1^\dagger \hat{a}_1} = \sum_{n=0}^{\infty} \frac{\ln^n g}{n!} (\hat{a}_1^\dagger \hat{a}_1)^n, \quad (30)$$

where the amplification gain satisfies $g \rightarrow \sqrt{(V+1)/(V-1)}$. The NLA defined above cannot be realized as it does not converge as n grows but approximation to the NLA is possible.

Our analytical solution to the CF of multi-mode Gaussian states is limited to generalized PV operations, i.e., the superposition of either photon subtraction or addition. For general non-Gaussian operations that are polynomials of both ladder operators the solution to the CF is yet to be found. However, when applied to Gaussian states with symmetrical properties, the general non-Gaussian operations are equivalent to certain

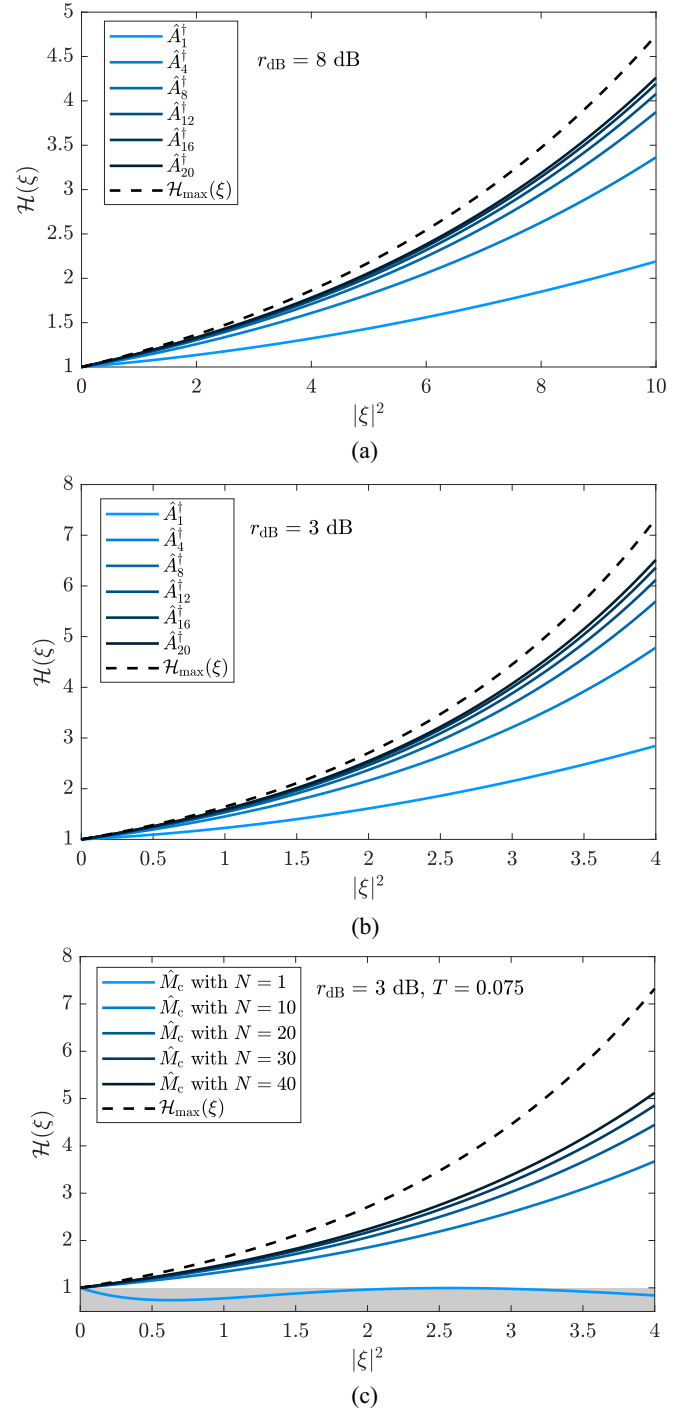


FIG. 4. (a) The response ratio functions $\mathcal{H}(\xi)$ for TMSV states with generalized PV operations defined by Eq. (26) with different parameter vector \mathbf{e} , where \mathbf{e} is set such that the integrated response ratio function is maximized. TMSV states with lower initial squeezing are considered in (b). In (c) the PC-NLA is considered. In all figures, the upper bound to the response ratio function $\mathcal{H}_{\text{max}}(\xi)$ is defined in Eq. (25). For solid curves, the value of N rises for curves from the bottom to the top.

generalized PV operations. For example, the identity

$$\frac{1}{\sqrt{V+1}} \hat{a}_2^\dagger |\text{TMSV}\rangle = \frac{1}{\sqrt{V-1}} \hat{a}_1 |\text{TMSV}\rangle, \quad (31)$$

and the commutation relation [69]

$$(\hat{a}_1^\dagger \hat{a}_1)^n = \sum_{m=1}^n \frac{1}{m!} \sum_{j=1}^m \binom{m}{j} (-1)^{m-j} j^n (\hat{a}_1^\dagger)^m \hat{a}_1^m, \quad (32)$$

show that any polynomials of $(\hat{a}_1^\dagger \hat{a}_1)$ with degree N can be mapped to an equivalent operator \hat{A}_N^\dagger (or \hat{A}_N) when applied to TMSV states. Therefore, on the one hand, for TMSV states, our solution can be used to analyze the impact of any non-Gaussian operations that are polynomials of the ladder operators, including the NLA and its approximations. On the other hand, the generalized PV operations \hat{A}_N^\dagger for TMSV states can be realized indirectly by known methods that approximate the NLA, e.g., coherent PV operations [70] or photon catalysis.

We use the NLA built from photon catalysis, which we refer to as PC-NLA, as a practical example to illustrate how the upper bound on $\mathcal{H}(\xi)$ can be approximated. It is worth noting that the PC-NLA, which requires a parallel application of single-photon photon catalysis [71], has been shown to improve the log-negativity of entangled states distributed over lossy channels. When applied to mode 1 of a TMSV state, the PC-NLA can be represented by an operator

$$\hat{M}_c = \sqrt{T}^{N+\hat{a}_1^\dagger \hat{a}_1} \sum_{k=0}^N \binom{N}{k} \left(\frac{T-1}{TN} \right)^k \hat{a}_1^{\dagger k} \hat{a}_1^k, \quad (33)$$

where N is the number of photon catalysis in the operation and $0 < T < 1$ is the beam-splitter transmissivity for each photon catalysis operation. More details on the PC-NLA can be found in Appendix B. Figure 4(c) compares the response ratio function $\mathcal{H}(\xi)$ associated with \hat{M}_c for different N , where we assume a phase correction operation $(-1)^{\hat{a}_1^\dagger \hat{a}_1}$ is applied to the TMSV state before the application of \hat{M}_c . Results in Fig. 4(c) show that the PC-NLA always provides increasing $\mathcal{H}(\xi)$ as N grows. However, for PC-NLA the function $\mathcal{H}(\xi)$ converges much slower to the bound compared with \hat{A}_N^\dagger with optimized parameters, suggesting PC-NLA is not the optimal method to approach the bound.

IV. TELEPORTATION WITH OTHER RESOURCE STATES AND PHOTON-VARYING OPERATIONS

In this section, we extend our studies of the PV operations to some generalized forms of TMSV states.

A. Two-mode squeezed coherent states

Two-mode squeezed coherent (TMSC) states have drawn research attention in recent years due to their ability to improve measurement-independent quantum key distribution [18,72,73]. A general TMSC state can be defined by [74]

$$|\text{TMSC}\rangle = \hat{D}_1(z_1) \hat{D}_2(z_2) \hat{S}(r) |0, 0\rangle_{1,2}, \quad (34)$$

where $\hat{D}_1(z_1)$, $\hat{D}_2(z_2)$ are displacement operators with $z_1, z_2 \in \mathbb{C}$. The above state has an alternative definition, which is given by swapping the order of the squeezing operator and the displacement operators

$$|\text{TMSC}\rangle = \hat{S}(r) \hat{D}_1(\tilde{z}_1) \hat{D}_2(\tilde{z}_2) |0, 0\rangle_{1,2}, \quad (35)$$

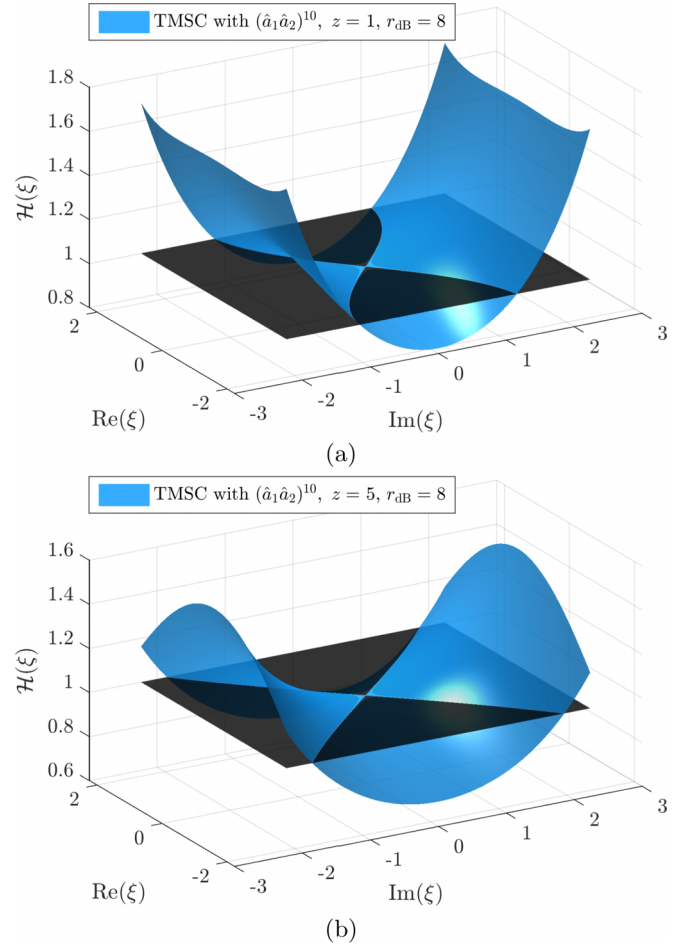


FIG. 5. The response ratio functions for two-mode squeezed coherent states with PV operations are shown in (a) and (b) with different displacement z . Both functions are symmetric with respect to the imaginary axis $\text{Im}(\xi)$.

where $\tilde{z}_1 = z_1 \cosh r - z_2^* \sinh r$ and $\tilde{z}_2 = z_2 \cosh r - z_1^* \sinh r$. In this work, we will use the definition in Eq. (34). The CF for a TMSC state can then be written as

$$\chi_{\text{TMSC}}(\xi_1, \xi_2) = e^{\xi_1 z_1^\dagger - \xi_1^\dagger z_1} e^{\xi_2 z_2^\dagger - \xi_2^\dagger z_2} \chi_{\text{TMSV}}(\xi_1, \xi_2), \quad (36)$$

where $\chi_{\text{TMSV}}(\xi_1, \xi_2)$ is the CF for the TMSV state in Eq. (20).

Consider the case for $z_1 = z_2 = z \in \mathbb{R}$, the response function for a TMSC state equals that of a TMSV state, $\chi_{\text{TMSV}}(\xi, \xi^*)$. Similar to before, the response ratio functions $\mathcal{H}(\xi)$ for TMSC states with PV operations can be calculated using Eq. (14), which are not shown here for conciseness. Examples of $\mathcal{H}(\xi)$ are shown in Figs. 5(a) and 5(b), where we have adopted a three-dimensional (3D) plot as they cannot be expressed as a function of $|\xi|$. Figure 5 shows that for a given PV operations $\mathcal{H}(\xi)$ decreases as z increases.

Next, we consider TMSC states with generalized PV operations \hat{A}_N^\dagger . Recall from Eq. (25) the upper bound to states with the response function $\chi_{\text{TMSV}}(\xi, \xi^*)$ is a polynomials of $|\xi|^2$. For \hat{A}_N^\dagger the non- $|\xi|^2$ terms in $\mathcal{H}(\xi)$ can also be eliminated by a proper setting of the parameter vector e . Figure 6(a) shows the optimized response ratio function for the TMSC states with different displacement z , where $\mathcal{H}(\xi)$ is optimized over e independently for each state. Similar to the results in

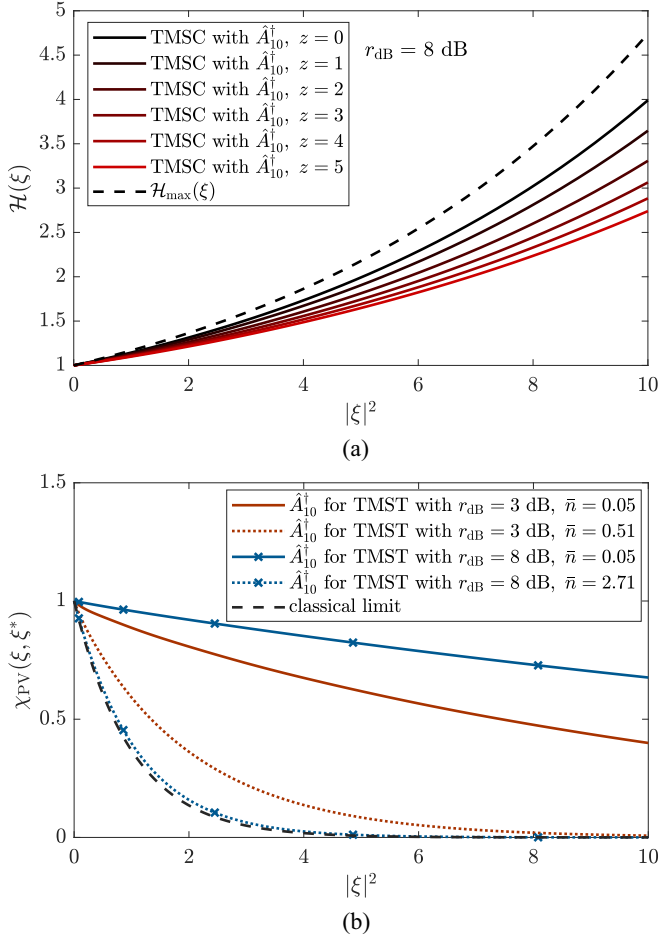


FIG. 6. (a) The response ratio function $\mathcal{H}(\xi)$ with generalized PV operations \hat{A}_N^\dagger (with $N = 10$) and optimized e for two-mode squeezed coherent states. For the solid curves, the value of z decreases for curves from the bottom to the top. (b) The response function $\chi_{\text{PV}}(\xi, \xi^*)$ for two-mode squeezed thermal states with generalized PV operation \hat{A}_{10}^\dagger .

Fig. 5, the $\mathcal{H}(\xi)$ for TMSC states with the generalized PV operations also decreases with increasing z . The results shown suggest that to obtain the maximal improvement offered by the generalized PV operations, the mean values of TMSC states must be displaced to zero before the operations.

B. Two-mode squeezed thermal states

Two-mode squeezed thermal (TMST) states are another generalization of the TMSV states. A TMST state can be defined by

$$\hat{\rho}_{\text{TMST}} = \hat{S}(r)\hat{\rho}_{\text{th1}}\hat{\rho}_{\text{th2}}\hat{S}^\dagger(r), \quad (37)$$

where

$$\hat{\rho}_{\text{th}i} = \sum_{n=0}^{\infty} \frac{\bar{n}_i^n}{(\bar{n}_i + 1)^{n+1}} |n\rangle_i \langle n|_i, \quad (38)$$

$i = 1, 2$ and the $\hat{\rho}_{\text{th}i}$'s are thermal states with mean photon number \bar{n}_i . Consider the case for $\bar{n}_1 = \bar{n}_2 = \bar{n}$, the CF for the

TMST state can be written as

$$\chi_{\text{TMST}}(\xi_1, \xi_2) = e^{-\frac{1}{2}[V(|\xi_1|^2 + |\xi_2|^2) - \sqrt{V^2 - 1}(\xi_1 \xi_2 + \xi_1^* \xi_2^*)]} (2\bar{n} + 1). \quad (39)$$

Figure 6(b) shows the response function $\chi_{\text{PV}}(\xi, \xi^*)$ for the TMST states with \hat{A}_N^\dagger , where we optimize $\mathcal{H}(\xi)$ over e and calculate the corresponding $\chi_{\text{PV}}(\xi, \xi^*)$. We note $\chi_{\text{PV}}(\xi, \xi^*)$ other than $\mathcal{H}(\xi)$ is shown to better compare the impact of the initial squeezing and the noise level. For the dotted curves the noise level \bar{n} is set such that the initial TMST state provides a fidelity for teleportation of coherent states of $1/2$, i.e., $\chi_{\text{TMST}}(\xi, \xi^*) = \exp(-|\xi|^2)$. As \bar{n} increases $\chi_{\text{PV}}(\xi, \xi^*)$ decreases, showing that the generalized PV operations cannot reduce noise in the resource state. Although not displayed in the figures, the operation \hat{A}_N^\dagger always provides $\mathcal{H}(\xi) > 1$ for the parameters considered.

C. Dissipative TMSV states

The distribution of entangled states is a prerequisite for quantum teleportation. For TMSV states passed through dissipative environments, the generalized PV operations cannot be realized in a local fashion. Therefore, we only consider the case where the PV operations are applied before the channel transmission of the TMSV state. Consider two independent lossy channels modeled by beam splitters with transmissivity T_1 and T_2 . A TMSV state is first applied with a generalized PV operation, of which the two modes are then transmitted through the channels. We define a new function $\mathcal{H}'(\xi)$ as the ratio between the response function for a TMSV state first applied with a generalized PV operation and then distributed over the channels, and the response function for a TMSV state directly distributed over the channels. We find that $\mathcal{H}'(\xi) > 1$ is always satisfied for $T_1 = T_2$. For $T_1 \neq T_2$, $\mathcal{H}'(\xi)$ might drop below unit for certain area of ξ . The above results coincide with the conclusion in [8] that TMSV states with higher squeezing are more sensitive to channels with asymmetric losses.

V. CONCLUSION

In this paper, we built a framework for PV operations in the multimode setting, expressing the characteristic function of the photon-varied two-mode Gaussian state as a multi-variable multi-index Hermite-Gaussian function. Based on the framework built, we introduced the response ratio function, a performance metric suitable for arbitrary teleportation input states. For given resource states, the fidelity for any input states can be calculated from the response ratio function. We then proposed generalized PV operations and investigated the use of such operations in various Gaussian states. Our results show that the generalized PV operations approximating noiseless linear amplification provide the most improvement in teleportation with TMSV states. Utilizing the symmetrical property of TMSV states, we also analyze the impact of PC-NLA with the response ratio function method, exemplifying possible methods for implementing the generalized PV operations in real-world communication systems.

It is worth noting that the analytical solution derived in this work, the Hermite-Gaussian function, is limited to

non-Gaussian operations that are polynomials of either ladder operator. For more general non-Gaussian operations that are polynomials of both ladder operators, e.g., cascaded PV operations and photon catalysis, the solution is yet to be found. For non-Gaussian operations that cannot be represented by ladder operators, e.g., quantum scissors and their generalization [75,76], the corresponding characteristic function will not have a Hermite-Gaussian form. However, quantum scissors can still be analyzed using the response ratio method proposed in this work.

ACKNOWLEDGMENTS

The authors acknowledge financial support from China Postdoctoral Science Foundation (Fund No. 2023M741315) and self-determined research funds of CCNU from the colleges' basic research and operation of MOE (Fund No. CCNU23XJ014 and No. CCNU24JC009).

APPENDIX A: DERIVATIONS OF EQS. (9) AND (12)

The right side of Eq. (8) can be expanded to

$$e^{\mathbf{u}^T \mathbf{M} \mathbf{u} + \mathbf{x}^T \mathbf{u}} = \sum_{\{n_{i,j}\}, \{n_i\}} \left[\prod_{i=1}^{2K} \frac{(u_i^2 M_{i,i})^{n_{i,i}}}{n_{i,i}!} \right] \times \left[\prod_{i=1, j=i+1}^{2K} \frac{(u_i u_j 2M_{i,j})^{n_{i,j}}}{n_{i,j}!} \right] \left[\prod_{i=1}^{2K} \frac{(u_i x_i)^{n_i}}{n_i!} \right], \quad (\text{A1})$$

where the summation is taken with respect to the indices $n_{i,j}, n_i (1 \leq i \leq 2K, i \leq j \leq 2K)$ over $[0, \infty)$. Combing the u_i 's in the above equation leads to

$$e^{\mathbf{u}^T \mathbf{M} \mathbf{u} + \mathbf{x}^T \mathbf{u}} = \sum_{\{n_{i,j}\}, \{n_i\}} \left[\prod_{i=1, j=i+1}^{2K} \frac{M_{i,i}^{n_{i,i}} (2M_{i,j})^{n_{i,j}} x_i^{n_i}}{n_{i,i}! n_{i,j}! n_i!} \right] \times \prod_{i=1}^{2K} u_i^{n_i + n_{i,i} + \sum_{j'=1}^{2K} n_{\min(i,j'), \max(i,j')}}. \quad (\text{A2})$$

Let $n_i^* = n_i + n_{i,i} + \sum_{j'=1}^{2K} n_{\min(i,j'), \max(i,j')}$ and $q_i = n_i - n_{i,i} - \sum_{j'=1}^{2K} n_{\min(i,j'), \max(i,j')}$, both for $1 \leq i \leq 2K$, then the above equation can be rewritten as

$$e^{\mathbf{u}^T \mathbf{M} \mathbf{u} + \mathbf{x}^T \mathbf{u}} = \sum_{\{n_i^*\}} \prod_{i=1}^{2K} u_i^{n_i^*} \sum_{\{n_{i,j}\}} \left[\prod_{i=1}^{2K} \frac{n_i! x_i^{q_i} M_{i,i}^{n_{i,i}}}{q_i! n_{i,i}!} \prod_{j=i+1}^{2K} \frac{(2M_{i,j})^{n_{i,j}}}{n_{i,j}!} \right]. \quad (\text{A3})$$

Comparing the right side of the above equation and the left side of Eq. (8), we can then obtain the result in Eq. (9).

Let

$$f(\mathbf{x} - \mathbf{u}) = e^{-\frac{1}{2}(\mathbf{x}-\mathbf{u})^T \mathbf{M}(\mathbf{x}-\mathbf{u}) + \mathbf{d}^T(\mathbf{x}-\mathbf{u})}, \quad (\text{A4})$$

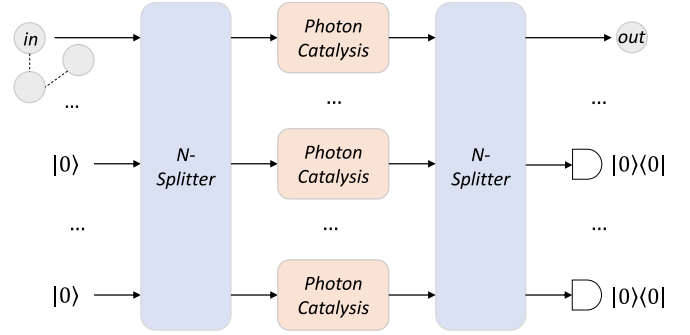


FIG. 7. The schematic for the PC-NLA. The photon catalysis shown in the paths is implemented using the device in Fig. 1(a) with $m = l = 1$.

denote the right side of Eq. (11), of which the Taylor expansion with respect to \mathbf{u} at 0 can then be written as

$$\sum_{n_1, \dots, n_{2K}=0}^{\infty} \left(\prod_{i=1}^{2K} \frac{u_i^{n_i}}{n_i!} \right) \frac{\partial^{\sum_{i=1}^{2K} n_i}}{\prod_{i=1}^{2K} (\partial u_i)^{n_i}} f(\mathbf{x} - \mathbf{u})|_{\mathbf{u}=0} = \sum_{n_1, \dots, n_{2K}=0}^{\infty} \left(\prod_{i=1}^{2K} \frac{u_i^{n_i}}{n_i!} \right) \frac{\partial^{\sum_{i=1}^{2K} n_i}}{\prod_{i=1}^{2K} (\partial x_i)^{n_i}} (-1)^{\sum_{i=1}^{2K} n_i} f(\mathbf{x}). \quad (\text{A5})$$

Comparing the right side of the above equation and the left side of Eq. (11), we can then obtain the result in Eq. (12).

APPENDIX B: PC-NLA

As is shown in Fig. 7, one major component of the PC-NLA is the N -splitter, which consists of an array of beam splitters. The first N -splitter, in conjunction with the vacuum ancillas, evenly divides the input state into N paths. Parallel photon catalysis operations are then applied to each path. The transmissivities T for the beam splitters in the photon catalysis operations are identical. The second N -splitter adopts an inverse to the arrangement of the beam splitters in the first N -splitter. The paths after the photon catalysis operations are recombined at the second N -splitter. The operation is successful when all the output ports except the first port of the second N -splitter register zero photons.

The PC-NLA can be represented by the operator [71]

$$\hat{M}_c = \sum_{n=0}^{\infty} \sqrt{T}^{N+n} \sum_{k=0}^N \binom{N}{k} \frac{n!}{(n-N+k)!} \left(\frac{p}{N}\right)^{N-k} |n\rangle \langle n|, \quad (\text{B1})$$

where $p = (T - 1)/T$, which can be rewritten as

$$\hat{M}_c = \sqrt{T}^{N+\hat{a}^\dagger \hat{a}} \sum_{k=0}^N \binom{N}{k} \left(\frac{p}{N}\right)^k \hat{a}^{\dagger k} \hat{a}^k. \quad (\text{B2})$$

To see how the above operation approximates the NLA, in the limit of $N \rightarrow \infty$, consider the application of \hat{M}_c on one mode

of a TMSV state with finite squeezing

$$\begin{aligned}
 \hat{M}_c |\text{TMSV}\rangle &= \sqrt{T^N(1-\lambda^2)} \sum_{n=0}^{N_c} (\sqrt{T}\lambda)^n \sum_{k=0}^{N_c} \frac{P^k \hat{a}_1^{\dagger k} \hat{a}_1^k}{k!} |n, n\rangle \\
 &= \sqrt{T^N(1-\lambda^2)} \sum_{n=0}^{N_c} (\sqrt{T}\lambda)^n \sum_{k=0}^n \binom{n}{k} P^k |n, n\rangle \\
 &= \sqrt{T^N(1-\lambda^2)} \sum_{n=0}^{N_c} (g\lambda)^n |n, n\rangle, \tag{B3}
 \end{aligned}$$

where N_c is a threshold set such that $N!/[(N-k)!k!N^k] \rightarrow 1/k!$ for $k < N_c$ and $\lambda^n \rightarrow 0$ for $n > N_c$, and $g = (2T - 1)/\sqrt{T} < -1$ for $T < 1/4$.

In teleportation using TMSV states, the minus sign of the amplification gain will result in a decrease in the

achievable teleportation fidelity. The sign can be corrected by applying two successive PC-NLA on one mode of a TMSV state, applying PC-NLA on both modes of the state, or simply applying a phase correction operation $(-1)^{\hat{a}^\dagger \hat{a}}$ on the state.

-
- [1] H. Yonezawa, T. Aoki, and A. Furusawa, Demonstration of a quantum teleportation network for continuous variables, *Nature (London)* **431**, 430 (2004).
- [2] X.-M. Jin, J.-G. Ren, B. Yang, Z.-H. Yi, F. Zhou, X.-F. Xu, S.-K. Wang, D. Yang, Y.-F. Hu, S. Jiang *et al.*, Experimental free-space quantum teleportation, *Nat. Photonics* **4**, 376 (2010).
- [3] X.-S. Ma, T. Herbst, T. Scheidl, D. Wang, S. Kropatschek, W. Naylor, B. Wittmann, A. Mech, J. Kofler, E. Anisimova *et al.*, Quantum teleportation over 143 kilometres using active feed-forward, *Nature (London)* **489**, 269 (2012).
- [4] J.-G. Ren, P. Xu, H.-L. Yong, L. Zhang, S.-K. Liao, J. Yin, W.-Y. Liu, W.-Q. Cai, M. Yang, L. Li *et al.*, Ground-to-satellite quantum teleportation, *Nature (London)* **549**, 70 (2017).
- [5] D. Lago-Rivera, J. V. Rakonjac, S. Grandi, and H. D. Riedmatten, Long distance multiplexed quantum teleportation from a telecom photon to a solid-state qubit, *Nat. Commun.* **14**, 1889 (2023).
- [6] J. Zhao, H. Jeng, L. O. Conlon, S. Tserkis, B. Shajilal, K. Liu, T. C. Ralph, S. M. Assad, and P. K. Lam, Enhancing quantum teleportation efficacy with noiseless linear amplification, *Nat. Commun.* **14**, 4745 (2023).
- [7] H. Vahlbruch, M. Mehmet, K. Danzmann, and R. Schnabel, Detection of 15 dB squeezed states of light and their application for the absolute calibration of photoelectric quantum efficiency, *Phys. Rev. Lett.* **117**, 110801 (2016).
- [8] M. Mičuda, I. Straka, M. Miková, M. Dušek, N. J. Cerf, J. Fiurášek, and M. Ježek, Noiseless loss suppression in quantum optical communication, *Phys. Rev. Lett.* **109**, 180503 (2012).
- [9] P. Huang, G. He, J. Fang, and G. Zeng, Performance improvement of continuous-variable quantum key distribution via photon subtraction, *Phys. Rev. A* **87**, 012317 (2013).
- [10] L. F. Borelli, L. S. Aguiar, J. A. Roversi, and A. Vidiellabarranco, Quantum key distribution using continuous-variable non-Gaussian states, *Quantum Info. Proc.* **15**, 893 (2016).
- [11] Z. Li, Y. Zhang, X. Wang, B. Xu, X. Peng, and H. Guo, Non-Gaussian postselection and virtual photon subtraction in continuous-variable quantum key distribution, *Phys. Rev. A* **93**, 012310 (2016).
- [12] Y. Guo, Q. Liao, Y. Wang, D. Huang, P. Huang, and G. Zeng, Performance improvement of continuous-variable quantum key distribution with an entangled source in the middle via photon subtraction, *Phys. Rev. A* **95**, 032304 (2017).
- [13] Y. Zhao, Y. Zhang, Z. Li, S. Yu, and H. Guo, Improvement of two-way continuous-variable quantum key distribution with virtual photon subtraction, *Quantum Info. Proc.* **16**, 184 (2017).
- [14] H.-X. Ma, P. Huang, D.-Y. Bai, S.-Y. Wang, W.-S. Bao, and G.-S. Zeng, Continuous-variable measurement-device-independent quantum key distribution with photon subtraction, *Phys. Rev. A* **97**, 042329 (2018).
- [15] Y. Guo, W. Ye, H. Zhong, and Q. Liao, Continuous-variable quantum key distribution with non-Gaussian quantum catalysis, *Phys. Rev. A* **99**, 032327 (2019).
- [16] L. Hu, M. Al-amri, Z. Liao, and M. S. Zubairy, Continuous-variable quantum key distribution with non-Gaussian operations, *Phys. Rev. A* **102**, 012608 (2020).
- [17] M. He, R. Malaney, and J. Green, Multi-mode CV-QKD with non-Gaussian operations, *Quantum Engineering* **2**, e40 (2020).
- [18] J. Singh and S. Bose, Non-Gaussian operations in measurement-device-independent quantum key distribution, *Phys. Rev. A* **104**, 052605 (2021).
- [19] X. Chen, F. Jia, T. Zhao, N. Zhou, S. Liu, and L. Hu, Continuous-variable quantum key distribution based on non-Gaussian operations with on-off detection, *Opt. Express* **31**, 32935 (2023).
- [20] X. Wang, M. Xu, Y. Zhao, Z. Chen, S. Yu, and H. Guo, Non-Gaussian reconciliation for continuous-variable quantum key distribution, *Phys. Rev. Appl.* **19**, 054084 (2023).
- [21] T. Ralph and A. Lund, Nondeterministic noiseless linear amplification of quantum systems, in *AIP Conference Proceedings*, Vol. 1110 (American Institute of Physics, Melville, NY, 2009), pp. 155–160.
- [22] H.-J. Kim, S.-Y. Lee, S.-W. Ji, and H. Nha, Quantum linear amplifier enhanced by photon subtraction and addition, *Phys. Rev. A* **85**, 013839 (2012).

- [23] S. Yang, S. L. Zhang, X. B. Zou, S. W. Bi, and X. L. Lin, Continuous-variable entanglement distillation with noiseless linear amplification, *Phys. Rev. A* **86**, 062321 (2012).
- [24] C. N. Gagatsos, J. Fiurášek, A. Zavatta, M. Bellini, and N. J. Cerf, Heralded noiseless amplification and attenuation of non-Gaussian states of light, *Phys. Rev. A* **89**, 062311 (2014).
- [25] S. Zhang and X. Zhang, Photon catalysis acting as noiseless linear amplification and its application in coherence enhancement, *Phys. Rev. A* **97**, 043830 (2018).
- [26] H. Adnane, M. Bina, F. Albarelli, A. Gharbi, and M. G. A. Paris, Quantum state engineering by nondeterministic noiseless linear amplification, *Phys. Rev. A* **99**, 063823 (2019).
- [27] J. Fiurášek, Teleportation-based noiseless quantum amplification of coherent states of light, *Opt. Express* **30**, 1466 (2022).
- [28] A. P. Lund and T. C. Ralph, Continuous-variable entanglement distillation over a general lossy channel, *Phys. Rev. A* **80**, 032309 (2009).
- [29] S. L. Zhang and P. van Loock, Distillation of mixed-state continuous-variable entanglement by photon subtraction, *Phys. Rev. A* **82**, 062316 (2010).
- [30] J. Fiurášek, Distillation and purification of symmetric entangled Gaussian states, *Phys. Rev. A* **82**, 042331 (2010).
- [31] A. Datta, L. Zhang, J. Nunn, N. K. Langford, A. Feito, M. B. Plenio, and I. A. Walmsley, Compact continuous-variable entanglement distillation, *Phys. Rev. Lett.* **108**, 060502 (2012).
- [32] J. Lee and H. Nha, Entanglement distillation for continuous variables in a thermal environment: Effectiveness of a non-Gaussian operation, *Phys. Rev. A* **87**, 032307 (2013).
- [33] S. L. Zhang, Y. L. Dong, X. B. Zou, B. S. Shi, and G. C. Guo, Continuous-variable-entanglement distillation with photon addition, *Phys. Rev. A* **88**, 032324 (2013).
- [34] K. P. Seshadreesan, H. Krovi, and S. Guha, Continuous-variable entanglement distillation over a pure loss channel with multiple quantum scissors, *Phys. Rev. A* **100**, 022315 (2019).
- [35] Y. Mardani, A. Shafiei, M. Ghadimi, and M. Abdi, Continuous-variable entanglement distillation by cascaded photon replacement, *Phys. Rev. A* **102**, 012407 (2020).
- [36] S. Ghose and B. C. Sanders, Non-Gaussian ancilla states for continuous variable quantum computation via Gaussian maps, *J. Mod. Opt.* **54**, 855 (2007).
- [37] K. Marshall, R. Pooser, G. Siopsis, and C. Weedbrook, Repeat-until-success cubic phase gate for universal continuous-variable quantum computation, *Phys. Rev. A* **91**, 032321 (2015).
- [38] K. Miyata, H. Ogawa, P. Marek, R. Filip, H. Yonezawa, J.-I. Yoshikawa, and A. Furusawa, Implementation of a quantum cubic gate by an adaptive non-Gaussian measurement, *Phys. Rev. A* **93**, 022301 (2016).
- [39] K. Marshall, C. S. Jacobsen, C. Schäfermeier, T. Gehring, C. Weedbrook, and U. L. Andersen, Continuous-variable quantum computing on encrypted data, *Nat. Commun.* **7**, 13795 (2016).
- [40] P. T. Cochrane, T. C. Ralph, and G. J. Milburn, Teleportation improvement by conditional measurements on the two-mode squeezed vacuum, *Phys. Rev. A* **65**, 062306 (2002).
- [41] F. Dell'Anno, S. De Siena, L. Albano, and F. Illuminati, Continuous-variable quantum teleportation with non-Gaussian resources, *Phys. Rev. A* **76**, 022301 (2007).
- [42] Y. Yang and F.-L. Li, Entanglement properties of non-Gaussian resources generated via photon subtraction and addition and continuous-variable quantum-teleportation improvement, *Phys. Rev. A* **80**, 022315 (2009).
- [43] F. Dell'Anno, S. De Siena, and F. Illuminati, Realistic continuous-variable quantum teleportation with non-Gaussian resources, *Phys. Rev. A* **81**, 012333 (2010).
- [44] K. P. Seshadreesan, J. P. Dowling, and G. S. Agarwal, Non-Gaussian entangled states and quantum teleportation of schrödinger-cat states, *Phys. Scr.* **90**, 074029 (2015).
- [45] X.-X. Xu, Enhancing quantum entanglement and quantum teleportation for two-mode squeezed vacuum state by local quantum-optical catalysis, *Phys. Rev. A* **92**, 012318 (2015).
- [46] S. Wang, L.-L. Hou, X.-F. Chen, and X.-F. Xu, Continuous-variable quantum teleportation with non-Gaussian entangled states generated via multiple-photon subtraction and addition, *Phys. Rev. A* **91**, 063832 (2015).
- [47] L. Hu, Z. Liao, and M. S. Zubairy, Continuous-variable entanglement via multiphoton catalysis, *Phys. Rev. A* **95**, 012310 (2017).
- [48] W. Ye, Y. Guo, H. Zhang, H. Zhong, Y. Xia, S. Chang, and L. Hu, Nonclassicality and entanglement properties of non-Gaussian entangled states via a superposition of number-conserving operations, *Quantum Info. Proc.* **19**, 1 (2020).
- [49] X.-G. Meng, K.-C. Li, J.-S. Wang, X.-Y. Zhang, Z.-T. Zhang, Z.-S. Yang, and B.-L. Liang, Continuous-variable entanglement and wigner-function negativity via adding or subtracting photons, *Ann. Phys. (Leipzig)* **532**, 1900585 (2020).
- [50] S. Bose and M. S. Kumar, Analysis of necessary and sufficient conditions for quantum teleportation with non-Gaussian resources, *Phys. Rev. A* **103**, 032432 (2021).
- [51] E. Villaseñor and R. Malaney, Enhancing continuous variable quantum teleportation using non-Gaussian resources, in *2021 IEEE Global Communications Conference (GLOBECOM)* (IEEE, New York, 2021), pp. 1–6.
- [52] T. Q. Dat and T. M. Duc, Entanglement, nonlocal features, quantum teleportation of two-mode squeezed vacuum states with superposition of photon-pair addition and subtraction operations, *Optik* **257**, 168744 (2022).
- [53] C. Kumar and S. Arora, Success probability and performance optimization in non-Gaussian continuous-variable quantum teleportation, *Phys. Rev. A* **107**, 012418 (2023).
- [54] T. M. Duc and T. Q. Dat, Enhanced entanglement and quantum teleportation of two-mode squeezed vacuum state via multi-stage non-Gaussian operations, *Optik* **287**, 170988 (2023).
- [55] H. S. Chuong and T. M. Duc, Enhancement of non-Gaussianity and nonclassicality of pair coherent states by superposition of photon addition and subtraction, *J. Phys. B: At., Mol. Opt. Phys.* **56**, acf484 205401 (2023).
- [56] E. R. Zinatullin, S. B. Korolev, and T. Y. Golubeva, Teleportation protocols with non-Gaussian operations: Conditional photon subtraction versus cubic phase gate, *Phys. Rev. A* **107**, 022422 (2023).
- [57] K. Sharma, B. C. Sanders, and M. M. Wilde, Optimal tests for continuous-variable quantum teleportation and photodetectors, *Phys. Rev. Res.* **4**, 022422 (2022).
- [58] H. K. Mishra, S. K. Oskouei, and M. M. Wilde, Optimal input states for quantifying the performance of CV unidirectional and bidirectional teleportation, *Phys. Rev. A* **107**, 062603 (2023).
- [59] M. Walschaers, S. Sarkar, V. Parigi, and N. Treps, Tailoring non-Gaussian continuous-variable graph states, *Phys. Rev. Lett.* **121**, 220501 (2018).
- [60] Y.-C. Su and S.-T. Wu, Entanglement enhancement through multirail noise reduction for continuous-variable

- measurement-based quantum-information processing, *Phys. Rev. A* **96**, 032327 (2017).
- [61] L. Vaidman, Teleportation of quantum states, *Phys. Rev. A* **49**, 1473 (1994).
- [62] S. L. Braunstein and H. J. Kimble, Teleportation of continuous quantum variables, *Phys. Rev. Lett.* **80**, 869 (1998).
- [63] P. Marian and T. A. Marian, Continuous-variable teleportation in the characteristic-function description, *Phys. Rev. A* **74**, 042306 (2006).
- [64] A. V. Chizhov, L. Knöll, and D.-G. Welsch, Continuous-variable quantum teleportation through lossy channels, *Phys. Rev. A* **65**, 022310 (2002).
- [65] S. Guerrini, M. Z. Win, and A. Conti, Photon-varied quantum states: Unified characterization, *Phys. Rev. A* **108**, 022425 (2023).
- [66] J. Niset, U. L. Andersen, and N. J. Cerf, Experimentally feasible quantum erasure-correcting code for continuous variables, *Phys. Rev. Lett.* **101**, 130503 (2008).
- [67] M. Lassen, M. Sabuncu, A. Huck, J. Niset, G. Leuchs, N. J. Cerf, and U. L. Andersen, Quantum optical coherence can survive photon losses using a continuous-variable quantum erasure-correcting code, *Nat. Photonics* **4**, 700 (2010).
- [68] M. Sabuncu, R. Filip, G. Leuchs, and U. L. Andersen, Environment-assisted quantum-information correction for continuous variables, *Phys. Rev. A* **81**, 012325 (2010).
- [69] P. Blasiak, A. Horzela, K. A. Penson, A. I. Solomon, and G. H. Duchamp, Combinatorics and boson normal ordering: A gentle introduction, *Am. J. Phys.* **75**, 639 (2007).
- [70] A. Chatterjee, H. S. Dhar, and R. Ghosh, Nonclassical properties of states engineered by superpositions of quantum operations on classical states, *J. Phys. B: At., Mol. Opt. Phys.* **45**, 205501 (2012).
- [71] M. He, R. Malaney, and B. A. Burnett, Noiseless linear amplifiers for multimode states, *Phys. Rev. A* **103**, 012414 (2021).
- [72] C. Kumar, J. Singh, S. Bose, Arvind, Coherence-assisted non-Gaussian measurement-device-independent quantum key distribution, *Phys. Rev. A* **100**, 052329 (2019).
- [73] W. Ye, Y. Guo, H. Zhang, S. Chang, Y. Xia, S. Xiong, and L. Hu, Coherent superposition of photon subtraction- and addition-based two-mode squeezed coherent state: Quantum properties and its applications, *Quantum Info. Proc.* **22**, 62 (2023).
- [74] M. Salvadoray and M. S. Kumar, Phase properties of correlated two-mode squeezed coherent states, *Opt. Commun.* **136**, 125 (1997).
- [75] M. S. Winnel, N. Hosseini-dehaj, and T. C. Ralph, Generalized quantum scissors for noiseless linear amplification, *Phys. Rev. A* **102**, 063715 (2020).
- [76] J. J. Guanzon, M. S. Winnel, A. P. Lund, and T. C. Ralph, Ideal quantum teleamplification up to a selected energy cutoff using linear optics, *Phys. Rev. Lett.* **128**, 160501 (2022).